Structure of the $K^\pi = 4^+$ bands in ^{186,188}Os

A. A. Phillips,[1] P. E. Garrett,[1,*] N. Lo Iudice,[2] A. V. Sushkov,[3] L. Bettermann,[4] N. Braun,[4] D. G. Burke,[5] G. A. Demand,[1] T. Faestermann,[6] P. Finlay,[1] K. L. Green,[1] R. Hertenberger,[7] K. G. Leach,[1] R. Krücken,[6] M. A. Schumaker,[1] C. E. Svensson,[1] H.-F. Wirth,[6] and J. Wong[1]

[1]*Department of Physics, University of Guelph, Guelph, Ontario, Canada N1G 2W1*

[2]*Dipartimento di Scienze Fisiche, Universitá di Napoli "Federico II" and Istituto Nazionale di Fisica Nucleare, Monte S Angelo, Via Cintia, I-80126 Napoli, Italy*

[3]*Bogoliubov Laboratory of Theoretical Physics, Joint Institute for Nuclear Research, 141980 Dubna, Russia*

[4]*Institut für Kernphysik, Universität zu Köln, D-50937 Köln, Germany*

[5]*Department of Physics and Astronomy, McMaster University, Hamilton, Ontario, Canada L8S 4M1*

[6]*Physik Department, Technische Universität München, D-85748 Garching, Germany*

[7]*Facultät für Physik, Ludwig-Maximilians-Universität München, D-85748 Garching, Germany*

(Received 14 May 2010; revised manuscript received 7 July 2010; published 22 September 2010)

The $(^3\mathrm{He}, d)$ single-proton stripping reaction has been performed on targets of ^{185,187}Re to investigate the structures of the 4_3^+ states in ^{186,188}Os. The experiment employed 30 MeV ^{3}He beams, and the reaction products were analyzed with a Q3D spectrograph. Absolute cross sections were determined at nine angles between 5° and 50° for states up to approximately 3 MeV in excitation energy. Large $\frac{5}{2}^+[402]_\pi + \frac{3}{2}^+[402]_\pi$ two-quasiparticle components are deduced for the 4_3^+ levels of both isotopes. Their magnitudes are in agreement with calculations performed using the quasiparticle phonon model, which predicts a coexistence of a large hexadecapole with a smaller, but sizable, γ-γ component in the 4_3^+.

DOI: 10.1103/PhysRevC.82.034321 PACS number(s): 21.10.Jx, 21.10.Re, 25.55.Hp, 27.70.+q

I. INTRODUCTION

The existence of multiphonon states in deformed nuclei has been a particularly controversial topic since the 1960s. The existence of the two-phonon γ vibration has been the focus of many studies where the $K^\pi = 4^+$ band is expected at approximately twice the energy of the $K^\pi = 2^+$ γ bandhead, and to have $B(E2; 4^+_{\gamma\gamma} \to 2^+_\gamma) \cong 2 \times B(E2; 2^+_\gamma \to 0^+_{\mathrm{gs}})$. Initial assignments of two-phonon structures were based on energy considerations and branching ratio measurements since absolute $B(E2)$ values were lacking. Evidence for the existence of a significant component of the $K^\pi = 4^+_{\gamma\gamma}$ state, through the measurement in ^{168}Er of enhanced $B(E2; 4^+_{\gamma\gamma} \to 2^+_\gamma)$ values, only became available in the early 1990s [1]. Following this pioneering work, there have been a limited number of examples where absolute $B(E2)$ values were measured and other contradictory data were absent, such as in ^{164}Dy [2], ^{166}Er [3,4], and ^{168}Er [5,6]. In many other cases, either the $B(E2)$ values have not been determined, or as in the Os isotopes discussed below, other contradictory data exist [7].

The vibrational nature of the first $K^\pi = 4^+$ bands in the osmium isotopes has been debated for several decades. Early works [8–13] proposed a two-phonon interpretation based on level energy ratios; however, the results of (t, α) transfer reactions studying ^{190,192}Os revealed large two-quasiparticle components consistent with a suggested single-phonon hexadecapole structure [14]. Further experiments, such as inelastic α and proton scattering [15,16], provided additional support for the one-phonon hexadecapole interpretation, as they indicated a single-step population of the 4_3^+ levels with an enhanced $B(E4)$ value. Later, detailed Coulomb excitation measurements performed on ^{186,188,190,192}Os extracted $B(E2; 4^+_3 \to 2^+_\gamma)$ values that were approximately twice as large as the $B(E2; 2^+_\gamma \to 0^+_{\mathrm{gs}})$ values, and were interpreted as evidence that the wave functions are dominated by two-phonon components [17,18]. An earlier single-proton transfer study did not perform angular distributions and published a single spectrum from the $^{187}\mathrm{Re}(^3\mathrm{He}, d)^{188}\mathrm{Os}$ reaction at 40° [7]. The $B(E2)$ values were confirmed through lifetime measurements [19], and they sparked considerable debate [7,20,21] over which component in the wave function is dominant. This debate has been dormant for several years, but recent theoretical developments may provide vital clues to the understanding of the 4_3^+ levels.

A new calculation focused on the ^{188,190,192}Os isotopes [22] was performed within the quasiparticle-phonon model (QPM). It refined and extended a previous one devoted to a global view [23]. This new calculation provides a good description of the single nucleon transfer results and obtains a 4^+ band composed of a large hexadecapole phonon and a smaller, but sizable, two-phonon-vibration state. Here, the QPM analysis has been extended also to ^{186}Os.

The aim of the present work is to provide new and unique data to help clarify the nature of the 4_3^+ wave functions, by studying the $^{185,187}\mathrm{Re}(^3\mathrm{He}, d)^{186,188}\mathrm{Os}$ reactions. These reactions are particularly favorable, since the ^{185,187}Re targets have the unpaired proton in the $\frac{5}{2}^+[402]_\pi$ Nilsson configuration, and the parallel coupling with the $\frac{3}{2}^+[402]_\pi$ configuration is predicted [23,24] to be a major component of a $K^\pi = 4^+$ hexadecapole state in this mass

*pgarrett@physics.uoguelph.ca

TABLE I. Energies and phonon structure of the lowest $K^\pi \neq 0^+$ QPM bandhead states in Os isotopes. Calculations for ^{186}Os are new to this work, while others along with the notation may be found in Ref. [22].

$^A X$	K^π	E_n^{expt} (MeV)	E_{QPM} (MeV)	$[\lambda\mu]_i$ $[(\lambda\mu)_i(\lambda\mu)_j]$	C_i^2 C_{ij}^2
^{186}Os					
	2^+	0.767	0.570	$[22]_1$	0.94
	4^+	1.3519	1.428	$[44]_1$	0.669
				$[(22)_1, (22)_1]$	0.278
^{188}Os					
	2^+	0.633	0.548	$[22]_1$	0.95
	4^+	1.279	1.312	$[44]_1$	0.58
				$[(22)_1, (22)_1]$	0.33
^{190}Os					
	2^+	0.557	0.562	$[22]_1$	0.90
	4^+	1.163	1.10	$[44]_1$	0.59
				$[(22)_1, (22)_1]$	0.33
^{192}Os					
	2^+	0.423	0.423	$[22]_1$	0.89
	4^+	1.163	0.913	$[44]_1$	0.674
				$[(22)_1, (22)_1]$	0.291

region. The ^{185,187}Re(^{3}He, d)^{186,188}Os reactions would thus be expected to populate the $K^\pi = 4^+$ states, and the measured cross sections can be used to infer the amplitudes of the $\frac{5}{2}^+[402]_\pi \otimes \frac{3}{2}^+[402]_\pi$ two-quasiparticle configuration, which can be compared with the most recent microscopic calculations [22].

II. THEORY

Microscopic QPM calculations have been performed for ^{186}Os in the same way as for ^{188,190,192}Os [22]. The main difference between these two sets of calculations is that the ^{186}Os calculations used a neutron effective charge of $e_{\text{eff}} = 0.2$ while the others used $e_{\text{eff}} = 0.1$ in order to obtain a good description of energy levels.

Table I gives the predicted phonon structure of the γ bandhead and the $K^\pi = 4^+$ state of interest in $^{186-192}$Os, while Table II lists the Nilsson configurations entering the dominant phonon components. These components are used for later comparison with experiment. Concerning ^{186}Os, the first $K^\pi = 2^+$ state is dominated by the γ phonon, with an admixture of 94%. The first $K^\pi = 4^+$ state, on the other hand, is calculated to have a hexadecapole phonon content of 67%, and a two-phonon γ vibration admixture of 28%. The latter amplitude is comparable to the one in ^{192}Os but somewhat smaller than in the other two Os isotopes. The remaining components account for less than 5%.

Table II shows that the γ vibration is predicted to have an admixture of 17% for the $\frac{5}{2}^+[402]_\pi \otimes \frac{1}{2}[400]_\pi$ configuration, which can be directly probed in the present transfer reaction. The hexadecapole state is predicted to have an admixture of 61% for the $\frac{5}{2}^+[402]_\pi \otimes \frac{3}{2}^+[402]_\pi$ configuration, which dominates the wave function.

TABLE II. Energies and quasiparticle structure of the dominant QRPA components of the lowest ^{186}Os $K^\pi \neq 0^+$ QPM bandhead states. Notation from Ref. [22].

$[\lambda\mu]_i$	E_i (MeV)	$[q_1q_2]_{\tau\tau'}$	ψ	φ	$N_{\nu_i}(q_1q_2)$
$[22]_1$	0.719	$[(512)\downarrow(510)\uparrow]_{nn}$	−0.584	−0.133	0.323
		$[(514)\downarrow(512)\downarrow]_{nn}$	0.307	0.089	0.086
		$[(512)\uparrow(510)\uparrow]_{nn}$	0.299	0.082	0.083
		$[(503)\uparrow(501)\uparrow]_{nn}$	0.210	0.030	0.043
		$[(505)\uparrow(503)\uparrow]_{nn}$	0.169	0.087	0.021
		$[(402)\uparrow(400)\uparrow]_{pp}$	0.479	0.242	0.171
		$[(404)\downarrow(402)\downarrow]_{pp}$	0.221	0.142	0.029
		$[(402)\downarrow(400)\uparrow]_{pp}$	−0.178	−0.092	0.023
$[44]_1$	1.798	$[(514)\downarrow(510)\uparrow]_{nn}$	−0.354	−0.045	0.123
		$[(512)\uparrow(512)\downarrow]_{nn}$	0.296	0.056	0.084
		$[(402)\uparrow(402)\downarrow]_{pp}$	0.786	0.105	0.607
		$[(404)\downarrow(400)\uparrow]_{pp}$	−0.184	−0.063	0.030

As shown in Table III, the QPM 4_3^+ to 2_2^+ $E2$ transition strength in ^{186}Os is at least a factor of 2 smaller than the experimental value. The same calculation yields the $E4$ matrix element $\mathcal{M}_4(J_i \to J_f)(efm^4) = 1181\ efm^4$, which is very similar to the values in the other Os isotopes [22].

III. EXPERIMENT

The (^{3}He, d) reactions were performed with 30 MeV ^{3}He beams from the tandem accelerator at the Maier Leibnitz Laboratory, Garching, Germany, with beam currents up to 1.2 μA. These beams bombarded the ^{185,187}Re targets, and the charged reaction products were distinguished, based on their momenta, with the Q3D spectrograph [26]. The target thickness values were determined, as outlined in Ref. [27], to be 74 and 82 μg/cm^2, respectively, for the ^{185,187}Re targets. The targets were prepared by vacuum evaporation of isotopically enriched samples, containing 96.7% and 98.7% ^{185,187}Re, onto 8 μg/cm^2 $^{\text{nat}}$C and 19 μg/cm^2 ^{12}C foils, respectively. A systematic uncertainty in the thickness determination is estimated to be ±2.5%. The particles were detected at the focal plane where a position-sensitive proportional counter, which used a cathode-foil readout, provided, in addition to the position information, ΔE-E measurements from which it was possible to deduce the particle type.

The Q3D spectrograph acceptance angle was set with movable slits to have a solid angle up to 11.6 msr, while the beam current was integrated by a Faraday cup to provide a normalization for cross-section measurements. A correction on the order of 5% was applied for dead-time effects in the

TABLE III. QPM vs experimental $E2$ transitions strengths. The data are taken from [25].

Nucleus		Expt. (W.u.)	QPM (W.u.)
^{186}Os	$B(E2; 2_2^+ \to 0_1^+)$	10.1 ± 0.4	10.0
	$B(E2; 4_3^+ \to 2_2^+)$	27 ± 9	10.9
	R_4	2.7 ± 1.0	1.09

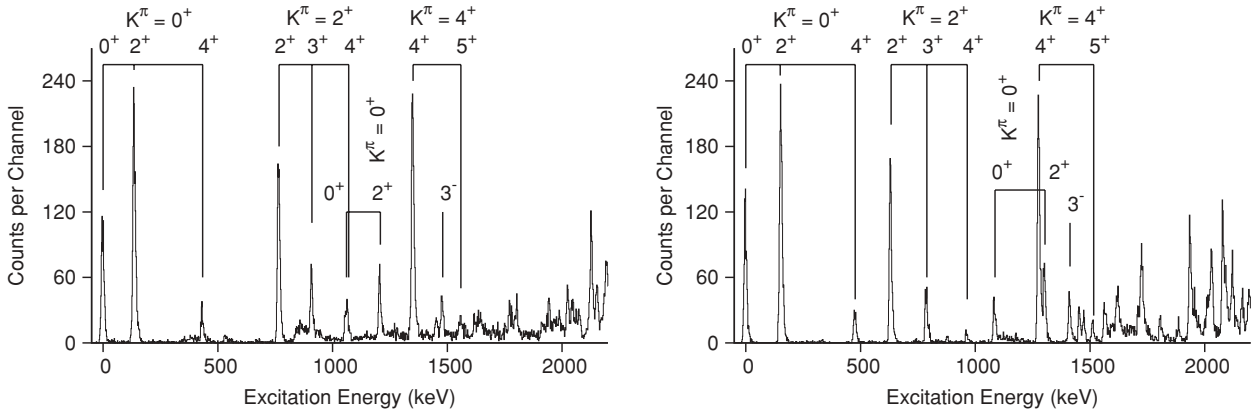

FIG. 1. Population of levels in ^{186}Os (left) and ^{188}Os (right) from (^{3}He, d) reactions with a 40° scattering angle.

detector and data acquisition system. The entire spectrograph was rotated through nine different angle settings, between 5° and 50°, to map out the cross sections as a function of angle. Two magnetic field settings of the spectrograph recorded data for states up to approximately 3 MeV in excitation energy. The typical resolution achieved ranged from 6.3 to 13.0 keV full width at half maximum (FWHM). Targets of Pt were used for an energy calibration above 1.5 MeV, under identical conditions, since the peaks from the ^{194,195}Pt(^{3}He, d)^{195,196}Au reactions are well known [28]. The energy uncertainty for strong, well-resolved peaks is approximately 1 keV, determined from both statistical uncertainty in the peak position and the uncertainty in the calibration polynomial.

IV. RESULTS

Sample spectra from the ^{185,187}Re(^{3}He, d)^{186,188}Os reactions are shown in Fig. 1. The spectra were fitted with the program GF3 from the RADWARE software package [29]. The global peak-shape parameters, the FWHM of the Gaussian, and the parameters for the exponential tail were fixed using a least-squares fit of the data up to a second-degree polynomial. Peak areas were transformed into cross sections using the target thickness, beam current, and Q3D solid angle.

The kinematics of the (^{3}He, d) reaction are such that at large angles, in the present case above 35°, the deuterons from the ^{185,187}Re(^{3}He, d)^{186,188}Os reactions are well separated from those originating from lighter-mass impurities present in the target or the backing. However, as small angles are approached, the prolific reactions on lighter-mass target components, such as C, can result in broad, irregularly shaped peaks in the spectrum that make extraction of accurate cross sections in some regions of the spectrum impossible. Figure 2 displays angular distributions for some low-lying states in ^{186,188}Os, where data points affected by impurity peaks have been removed. The curves shown are the result of distorted-wave Born approximation (DWBA) calculations, described below, for the transferred ℓ value indicated.

The DWBA calculations were performed with standard published sets of optical model parameters [28,30] using the DWUCK4 program [31]. The parameter set from Ref. [30] was used without a radial cutoff and without nonlocal and finite-range corrections. The data are well described by both sets of parameters, but the set from Ref. [28] matches the shape better.

It is noteworthy that the angular distributions for transfer into the ^{186,188}Os ground states, as shown in Fig. 2, which must be the result of a single ℓ transfer, are very well described. In addition, the transfer into the 2^+ member of the ground-state band, and the $I, K^\pi = 2, 2^+$ γ bandhead, are also well reproduced by the DWBA curve for $\ell = 2$ and $\ell = 0$, respectively. These results provide confidence that the (^{3}He, d) reactions at the beam energies employed do not have significant contributions from multistep processes.

The spectroscopic strengths, S_ℓ, were calculated by scaling DWBA calculations to the measured transfer cross sections according to the formula

$$S_\ell = \frac{\frac{d\sigma}{d\Omega}\big|_{\text{expt}}}{[N\frac{d\sigma}{d\Omega}(\theta, \ell, j)]_{\text{DWBA}}}, \quad (1)$$

where the numerator is the measured cross section, and the denominator is the normalized DWBA calculation. While in principle the transfer can occur for any j and ℓ values that satisfy parity and angular-momentum selection rules, it is observed that the experimental angular distributions appear to be dominated by a single ℓ transfer, and thus the reported spectroscopic strengths are the result of a fit with a single ℓ value. Although there is evidence that the Os isotopes possess softness in the γ degree of freedom, especially for $A > 190$, the Nilsson model with axial symmetry is employed to extract the amplitudes of the two-quasiparticle configurations in the ground-state, γ-vibrational, and $K^\pi = 4^+$ bands in both ^{186,188}Os. The spectroscopic strengths reported in Fig. 2 are an average of those obtained using the optical model parameters from Refs. [28,30]. A typical ±30% systematic uncertainty was adopted in all spectroscopic strengths reported.

Predictions for the cross sections for two-quasiparticle states were performed with the program EVE [32] that uses the Nilsson model calculations as outlined by Chi [33]. The values of κ and μ were taken to be 0.0637 and 0.600 [34]. The deformation δ_2 was set to 0.2, and the U^2 pairing factors were determined using the BCS formalism, with the quasiparticle

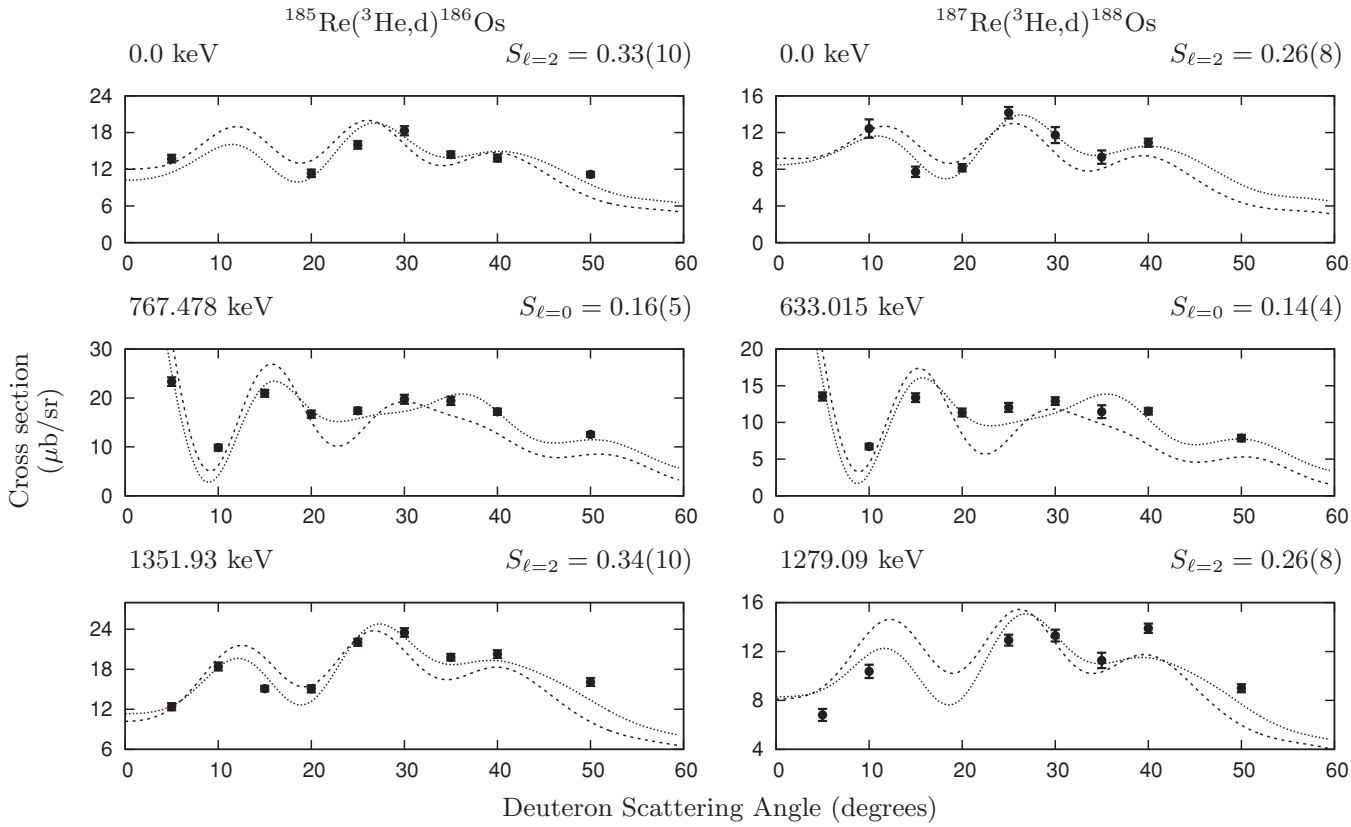

FIG. 2. Cross section measurements (μb/sr) compared with DWBA calculations for a single ℓ transfer. The dashed and dotted lines represent the optical model parameter sets from Ref. [30] and Ref. [28], respectively. The average spectroscopic strength is reported with a $\pm$30% systematic uncertainty.

energies taken from ^{185,187}Re and the gap parameter estimated using mass differences, outlined in Ref. [35]. In principle, Coriolis mixing can produce significant changes in the wave-function amplitudes; however, in the present case, the lack of requisite $\Delta K = 1$ bands in proximity to these states results in a negligible or insignificant perturbation, and the amplitudes of the Nilsson components are extracted by scaling the observed cross sections to those predicted using Eq. (2),

$$\frac{d\sigma}{d\Omega} = g^2 \sum_{j,\ell} C^2_{j,\ell} P^2 |\langle I_i K_i j \Delta K | I_f K_f \rangle|^2 \times \left[N \frac{d\sigma}{d\Omega}(\theta, \ell, j) \right]_{\mathrm{DWBA}}, \quad (2)$$

where $C_{j,\ell}$ is an amplitude in the spherical shell-model basis of a Nilsson wave-function component, and P^2 is a pairing occupancy factor (U^2 for stripping and V^2 for pickup, except for population of the ground-state band [36]). The Clebsch-Gordan coefficient accounts for the coupling of the transferred proton angular momentum (j, ΔK) to the initial state (I_i, K_i) yielding the final state (I_f, K_f). If the initial or final state is a paired $K = 0$ configuration, then $g^2 = 2$, otherwise $g^2 = 1$.

TABLE IV. Comparison of squared amplitudes of two-quasiparticle components from experiment using EVE calculations to the QPM predictions.

I^π	K^π	Configuration	Experiment		QPM	
			^{186}Os	^{188}Os	^{186}Os	^{188}Os
2	2	$\frac{5}{2}^+[402]_\pi - \frac{1}{2}^+[400]_\pi$	0.33(10)	0.28(8)	0.16	0.10
4	4	$\frac{5}{2}^+[402]_\pi + \frac{3}{2}^+[402]_\pi$	0.34(10)	0.27(9)	0.41	0.32

Using the above procedure with EVE calculations, the two-quasiparticle admixtures were extracted for the ground-state band $\frac{5}{2}^+[402]_\pi - \frac{5}{2}^+[402]_\pi$, the γ-vibrational band $\frac{5}{2}^+[402]_\pi - \frac{1}{2}^+[400]_\pi$, and $K^\pi = 4^+$ $\frac{5}{2}^+[402]_\pi + \frac{3}{2}^+[402]_\pi$ components. The ground-state $\frac{5}{2}^+[402]_\pi - \frac{5}{2}^+[402]_\pi$ squared amplitudes were determined to be 1.5(4) and 1.3(4) in ^{186,188}Os and are consistent with the expected value of unity for a Nilsson configuration dominated by a single j, ℓ value. The squared amplitudes for the γ-vibrational and the $K^+ = 4^+$ bandheads in ^{186,188}Os are listed in Table IV together with the QPM values.

V. CONCLUSIONS

The deduced admixtures of the two-quasiparticle components observed in the 4^+_3 levels are in good agreement with the QPM calculations [22], while there is about a factor of 2–3 difference when comparison is made for the γ-vibration bandhead. This difference between measurement and calculation

for the γ bandhead is significant but not unexpected, because the calculations are predicting the $\frac{5}{2}^+[402]_\pi - \frac{1}{2}^+[400]_\pi$ component to be one of the many small components of the entire wave function, whereas the $\frac{5}{2}^+[402]_\pi + \frac{3}{2}^+[402]_\pi$ component in the 4_3^+ state represents a large one.

Thus, the present data provide additional support to the QPM finding that the 4_3^+ states in Os isotopes, and in particular in ^{186,188}Os, are composed of a dominant single-hexadecapole component *and* a smaller yet important $\gamma\gamma$ admixture. This two-component view is able to explain both this work and the earlier transfer work, inelastic scattering results, and $B(E2)$ values.

It remains to explain why the QPM underestimates the $E2$ 4_3^+ to 2_2^+ transition strength in ^{186}Os. This discrepancy, similar to the one found in ^{192}Os [22], suggests that the two-phonon component should be somewhat larger, at least in these two nuclei. A moderate enhancement of such a component should not spoil the agreement with the present transfer data (Table IV). A specific theoretical investigation is needed to find a way of enhancing such a strength. Apart from this discrepancy, all data fit into the QPM scheme where both one- and two-phonon components coexist in the 4_3^+ states. Such a picture, supported by the present data, provides the key to reconciling the apparent conflict between transfer data and $B(E2)$ value measurements.

ACKNOWLEDGMENTS

We thank the beam operators and staff of the Maier Leibnitz Laboratory for their hard work and hospitality during the course of this work. We thank Dr. John Wood for his comments on this manuscript. This work was partially supported by the Natural Sciences and Engineering Research Council of Canada.

[1] H. G. Börner, J. Jolie, S. J. Robinson, B. Krusche, R. Piepenbring, R. F. Casten, A. Aprahamian, and J. P. Draayer, Phys. Rev. Lett. **66**, 691 (1991).
[2] F. Corminboeuf, J. Jolie, H. Lehmann, K. Föhl, F. Hoyler, H. G. Börner, C. Doll, and P. E. Garrett, Phys. Rev. C **56**, R1201 (1997).
[3] C. Fahlander, A. Axelsson, M. Heinebrodt, T. Härtlein, and D. Schwalm, Phys. Lett. B **388**, 475 (1996).
[4] P. E. Garrett, M. Kadi, M. Li, C. A. McGrath, V. Sorokin, M. Yeh, and S. W. Yates, Phys. Rev. Lett. **78**, 4545 (1997).
[5] M. Oshima *et al.*, Phys. Rev. C **52**, 3492 (1995).
[6] T. Härtlein, M. Heinebrodt, D. Schwalm, and C. Fahlander, Eur. Phys. J. A **2**, 253 (1998).
[7] D. G. Burke, AIP Conf. Proc. **529**, 216 (2000).
[8] H. L. Sharma and N. M. Hintz, Phys. Rev. Lett. **31**, 1517 (1973).
[9] H. L. Sharma and N. M. Hintz, Phys. Rev. C **13**, 2288 (1976).
[10] S. W. Yates, J. C. Cunnane, P. J. Daly, R. Thompson, and R. K. Sheline, Nucl. Phys. A **222**, 276 (1974).
[11] S. W. Yates, J. C. Cunnane, R. Hochel, and P. J. Daly, Nucl. Phys. A **222**, 301 (1974).
[12] R. F. Casten and J. A. Cizewski, Nucl. Phys. A **309**, 477 (1978).
[13] R. F. Casten and J. A. Cizewski, Nucl. Phys. A **425**, 653 (1984).
[14] R. D. Bagnell, Y. Tanaka, R. K. Sheline, D. G. Burke, and J. D. Sherman, Phys. Lett. B **66**, 129 (1977).
[15] D. G. Burke, M. A. M. Shahabuddin, and R. N. Boyd, Phys. Lett. B **78**, 48 (1978).
[16] F. T. Baker, A. Sethi, V. Penumetcha, G. T. Emery, W. P. Jones, M. A. Grimm, and M. L. Whiten, Nucl. Phys. A **501**, 546 (1989).
[17] M. Oshima *et al.*, Nucl. Phys. A **557**, 635 (1993).
[18] C. Y. Wu *et al.*, Nucl. Phys. A **607**, 178 (1996).
[19] C. Y. Wu *et al.*, Phys. Rev. C **64**, 014307 (2001).
[20] D. Burke, Phys. Rev. C **66**, 039801 (2002).
[21] C. Y. Wu *et al.*, Phys. Rev. C **66**, 039802 (2002).
[22] N. Lo Iudice and A. V. Sushkov, Phys. Rev. C **78**, 054304 (2008).
[23] V. O. Nesterenko, V. G. Solov'ev, A. V. Sushkov, and N. Yu. Shirikova, Sov. J. Nucl. Phys. **44**, 938 (1986).
[24] R. D. Bagnell, Y. Tanaka, R. K. Sheline, D. G. Burke, and J. D. Sherman, Phys. Rev. C **20**, 42 (1979).
[25] C. M. Baglin, Nucl. Data Sheets **99**, 1 (2003).
[26] M. Löffler, H. J. Scheerer, and H. Vonach, Instrum. Methods **111**, 1 (1973).
[27] P. E. Garrett *et al.*, Phys. Rev. C **79**, 017601 (2009).
[28] H.-F. Wirth *et al.*, Phys. Rev. C **70**, 014610 (2004).
[29] D. Radford, RADWARE software package, [http://radware.phy.ornl.gov].
[30] M. T. Lu and W. P. Alford, Phys. Rev. C **3**, 1243 (1971).
[31] P. D. Kunz, DWUCK4 computer code, University of Colorado (unpublished).
[32] R. O'Neil and R. Hirning, EVE computer code, McMaster University (unpublished).
[33] B. E. Chi, Nucl. Phys. **83**, 97 (1966).
[34] I.-L. Lamm, Nucl. Phys. A **125**, 504 (1969).
[35] J. Dobaczewski, P. Magierski, W. Nazarewicz, W. Satuła, and Z. Szymański, Phys. Rev. C **63**, 024308 (2001).
[36] D. G. Burke and B. Elbeck, Mat. Fys. Medd. K. Dan. Vidensk. Selsk. **36**, 1 (1967).